Archives of Hydro-Engineering and Environmental Mechanics 71 (2024), pp. 43–57, doi: 10.2478/heem-2024-0003

sciendo

ARCHIVES OF HYDRO-ENGINEERING AND ENVIRONMENTAL MECHANICS

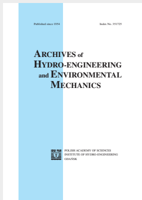

Published since 1954 ISSN 1231–3726

Analysis of Pluviograms Recorded in the Area of a Phosphogypsum Heap at Wiślinka, Poland

Aleksandra Korzec

Institute of Hydro-Engineering, Polish Academy of Sciences, Poland, ul. Kościerska 7, 80-328 Gdańsk;
e-mail: a.korzec@ibwpan.gda.pl

(Received 07 January 2024; revised 16 May 2024)

Abstract. The paper is devoted to the long-term project concerning monitoring and stability analysis of a 40 m high phosphogypsum heap located at Wiślinka, Poland. The research presented in the paper focused on collecting and processing rainfall data, which subsequently allows us to perform numerical simulation of rainfall impact on heap's behaviour. Such analysis requires time history of rainfall intensity, that is recorded by an automatic precipitation station. Since this is not common monitoring equipment, the characteristics of the station installed in the immediate vicinity of the heap are presented, and the data obtained in two experiments conducted in the laboratory are discussed. The analysis revealed that differences between introduced and measured total rain are as large as 10% for very heavy rains. Moreover, the recorded maximum rainfall intensity often includes errors. The data processing procedure to obtain time history of rainfall intensity is presented on the basis of data collected in the first half of the hydrological year 2023 (the first period of the station's operation). The total precipitation registered was 107 mm, and the maximum daily rain was only 26 mm. However, first single and multi-stage rainfall models for the Wiślinka region that would be applied into numerical simulations are presented.

Key words: precipitation; rainfall; rainfall gauge; pluviogram; rainfall intensity

List of Symbols

- q_t – maximum rainfall intensity in recording interval (one-minute), [mm/h];
- q_I – average rainfall intensity of rainfall event I, [mm/h];
- r – total rain in given time interval related to one square meter of ground surface projection, [mm];
- r_I – total rain of rainfall event I, [mm];
- r_t – current rain referred to recording interval (one-minute), [mm];
- r_Σ – total rain recorded in given time period, e.g. 3, 7 or 30 days, [mm];
- t_I – duration of rainfall event I, [min];
- t_N – absolute time, e.g. [h] or [day]
- μ – mean value.

1. Introduction

It is common knowledge that both global and local slope stability can be affected by rainfall, see e.g. Alonso et al (1996), Bednarczyk (2018), Cai and Ugai (2004), Corominas and Moya (1999), Zabuski et al (2015). Attempts have been made to perform numerical analyses of such impacts (Świtała and Wu 2019); however, the data required to determine the boundary condition is rarely available. To analyse long-term stability, information on annual precipitation obtained from daily recorded data is sufficient. Such data is commonly collected by meteorological stations using volume or weighting rain gauge. On the other hand, for short-term stability analysis, the rainfall intensity pattern is crucial. Usually, for short rainfall events, a uniform rainfall intensity is introduced over a given period of time. In the case of rainfall lasting several days, various artificial pattern are applied (Suradi and Andy 2014). To make analysis reliable, this characteristic should be determined for the designed site using automatic precipitation gauge (tipping bucket rain gauge or weighing rain gauge).

The automatic precipitation station was installed in the close vicinity to the reclaimed phosphogypsum heap located in Wiślinka, in the Pruszcz Gdański district in northern Poland. The 40 m high heap was formed on an area of 26 ha in the years 1969–2009. The majority of heap's slope inclination is around 35 degrees. Data collected by displacement monitoring system established for the post-exploitation phase indicate the occurrence of mass movements. In addition, at least three periods of horizontal displacement acceleration have occurred to date. These observations were one of the premises for undertaking research work and expanding the monitoring system. Rainfall data will be analysed on an ongoing basis in the search of their correlation with the displacements of the heap slopes monitored at survey points and inclinometers. The data will also be used for the slope stability analysis. However, determining rainfall patterns for that kind of analysis requires multi-year data collection. The paper presents the first attempt to determine boundary condition reflecting one-day and multi-day rainfall for numerical simulations.

Firstly, the characteristics of the precipitation measurement station are presented. The recorded variables are then discussed based on the two experiments performed in a laboratory. Finally, the collected data for the period from November 2022 to April 2023 is analysed. A procedure for selecting rainfall events and their processing is proposed.

2. Characteristics of the Precipitation Station

Precipitation is defined as the liquid or solid products of the condensation of water vapour falling from clouds or deposited from air onto the ground (WMO 2014). It includes rain, hail, snow, dew, rime, hoar frost and fog precipitation. Since rainfall is the most important component of precipitation affecting the engineering structures, these terms are used interchangeably in this work. The total volume of precipitation (water or water equivalent in the case of solid forms) which reaches the ground in a given period of time is expressed in terms of a water column height (usually expressed in millimetres) that would cover a prescribed horizontal projection of the ground surface (usually one square meter). It is a basic characteristics of rainfall event. However, for many application, the rainfall intensity which describes the amount of water falling in given time (usually in one hour) is of interest. It also allows classification of rainfall events as light/slight (when intensity is less than 2 mm/h) or a violent/naval rain (when intensity exceeds 50 mm/h), (Met Office 2007).

Fig. 1. Atmospheric precipitation station installed at Wiślinka

The installed atmospheric precipitation station consisted of components offered by DeltaOHM, Fig. 1. The main elements of the station are a tipping bucket rain gauge with a heating system (HD2015R.K1) and a data logger equipped with transmission modules (HD33LMT.4). The station is autonomous, powered by a battery charged from solar panel (HD32WSF.S12 and OPZ30W). Only during winter time additional power source is needed for the heating system. Even though the rain gauge is maintenance-free, inspection visits are necessary to remove dirt from the funnel of the rain gauge and check its levelling, especially if the station is not fenced.

2.1. Tipping-bucket Rain Gauge

The HD2015R rain gauge is designed according to guidelines of the World Meteorological Organization (DeltaOHMb 2022, WMO 2014). The rain gauge was installed on a 1 m high mast delivered by DeltaOHM. The funnel collects precipitation from an area of 200 cm^2, Fig. 2a. The spikes protecting the device from birds were mounted around its perimeter. To ensure measurement during winter it is equipped with a heating system, which activates around +4°C. It can work properly in the temperature range −20°C to 70°C.

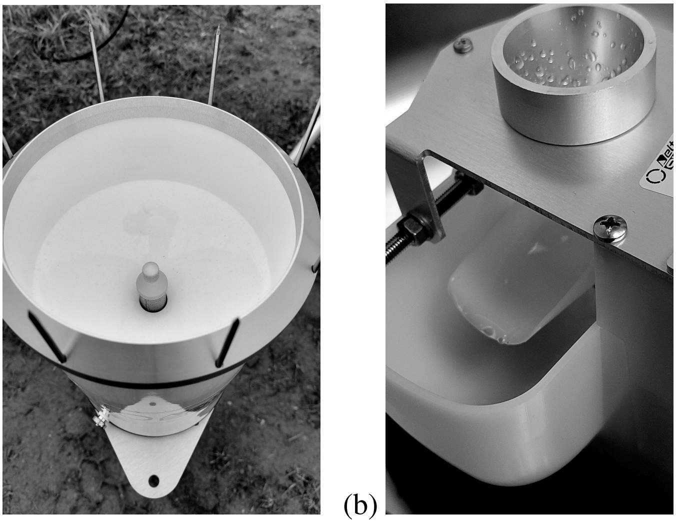

Fig. 2. (a) Active area (funnel), (b) bucket of HD2015 rain gauge by DeltaOHM

As the name of the tipping-bucket rain gauge suggests, the main element of the gauge consists of two interconnected containers which, like a seesaw, can be in two equilibrium positions. The water flows into the uppermost bucket. When the bucket is filled with a pre-set amount of water, it falls to the second equilibrium position and the water flows out of the device. Consequently, the water flows into the second bucket. Whenever the buckets change their positions, an electric pulse is sent to the SWIN1 analogue port of the data logger. The tipping bucket rain gauge resolution is limited to pre-set amount of precipitation that would cause a tip. Resolution is specified upon request between 0.1 mm, 0.2 mm and 0.5 mm. Due to the climate conditions in the installation spot, the 0.2 mm resolution was chosen. The certified average resolution of the installed rain gauge is 0.209 mm. However, accurate calculations should take into account the entire calibration curve delivered by manufacturer. It defines the amount of rain per one swing of gauge for rainfall intensity ranges from 10 mm/h to 200 mm/h. In our case the values vary from 0.198 mm to 0.224 mm. According to the specification, the maximum rainfall intensity that can be measured with this rain gauge is 600 mm/h.

It is deemed that tipping bucket underestimate the amount of rainfall, particularly in snowfall (evaporate due to heating) and heavy rainfall events (loss of water during the tipping action). However, daily records are less affected by evaporation than those recorded by graduated cylinders or weighing gauges. It is assumed that evaporation in summer time can reduce the daily rain up to 0,5 mm for that type of gauges.

2.2. Data Logger

The applied data logger is designed for weather station (DeltaOHMc 2022). The data logger was pre-set by the manufacturer in accordance with the purchased set of devices. The following rainfall parameters were set to be recorded: *current rain* r_t in mm, *max rain rate* in mm/h, *daily rain compensated* r_d in mm, and *total rain compensated* r in mm, which refer to an area of 1 m^2. The data are recorded at time interval set by the user. A one-minute interval was established. Thus, current rain recorded by a logger is equal to a rain that fell within one minute. The measurement is automatically modified by the recorder depending on the rainfall intensity using a calibration curve established experimentally by producer. For instance, for moderate rain (rate less than 10 mm/h), one tip means 0.198 mm, but for naval rain is equal to 0.224 mm. This approach requires the use of a larger number of data recorder channels for the rain gauge (at least two more, no information can be found in the manual). Unfortunately, the original records of pulses are not available.

Data can be sent via the mobile network to an ftp server, http server, and by e-mail. It was established that data is sent once a day to the fttp server by e-mail, and once every 15 minutes to www.deltaohm.cloud. Via web, the producer provides a useful application for data visualisation and downloading (DeltaOHMa 2022). The data format (.txt, .csv, .xls) and structure differs depending on the selected channel. Mostly, the data recording time step is not uniform. If a current rainfall value is zero for more than 30 minutes, no data is recorded. Regardless of the occurrence of rain, data is recorded for every full hour.

3. Tests

Because the data logger is pre-set and the pulse records are not available the tests were performed to understand what is exactly recorded by the data logger. Another reason was to check the user configuration. In the article, the test results are presented mainly to illustrate the available measurement results. However, the observations helped also to avoid wrong conclusions.

A. In the first test, the bucket was being tilted mechanically with a given frequency.
B. During the second test, the measurement was made with water of a known volume, which was dropped into the rain gauge at various flow rates.

3.1. Experiment A

Experiment A was conducted in four stages, in which the bucket was tilted at various frequencies, every 15 s, 5 s, 120 s and 45 s, respectively. A total of 187 pulses were generated. Assuming the average resolution of the device, total rain of 39.803 mm should be recorded.

The current rainfall time-history simulated during experiment A is presented in Fig. 3. Total rain, shown in Fig. 4, reached 40.809 mm. The difference between simulated and recorded values is within the stated device accuracy of 3%. The maximum rain rate time-history is presented in Fig. 5. The range of vertical axes is limited to the expected maximum rainfall intensity. Four intensities were calculated based on average resolution of the rain gauge.

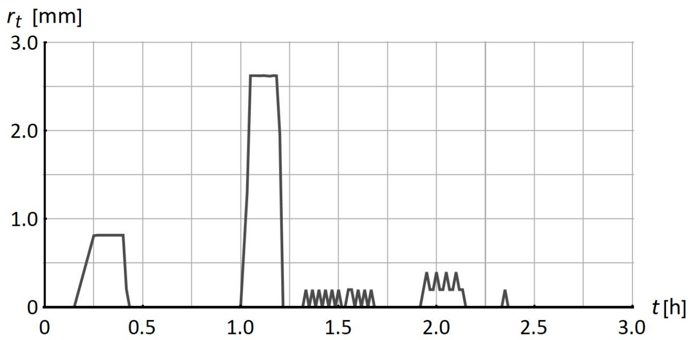

Fig. 3. Current rain time-history simulated during experiment A by mechanical tipping

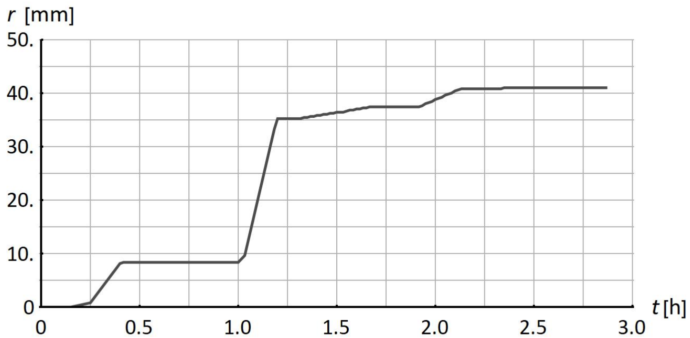

Fig. 4. Total rain compensated time-history simulated during experiment A

For each stages the minimum and maximum values of the current rain r_t were determined, as well as, maximum and average intensity of rainfall q_t. Moreover, total rainfall r_I and duration of rainfall t_I in stage I was determined. The average intensity

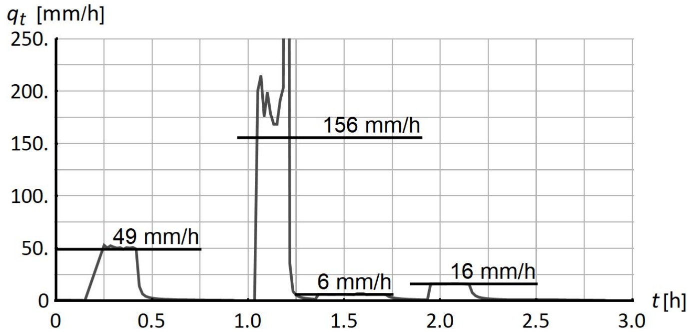

Fig. 5. Max rainfall rate time-history simulated during experiment A

of rainfall in stage I was also defined as r_I/t_I. Parameters determined are collected in Tab. 1. The results obtained for stage 1 and 4 of the experiment A are in good agreement with assumed parameters. The assumed rainfall intensities q_I were 50 mm/h and 17 mm/h, respectively. Both stages simulate heavy rain (Met Office 2007). In the third stage, when the condition of light rain was simulated (intensities equal to 6 mm/h) the difference reaches as much as 6%. In the case of the highest intensity (156 mm/h), stage 2, the records of q_t include 'overflow' flag and intensity values are much higher than assumed one, e.g. 1400 mm/h. The recorded value of q_t and the calculated average do not correspond to the experimental conditions performed. The intensity value calculated from the rainfall time history gives a correct picture, although is 10% higher than the expected average value. The raw data of pulses is not available; however, it seems possible, that above-mentioned unrealistic intensity values results from conversion of impulse records to one-minute intervals records. High intensity values may be obtained when the impulse occurred just after the beginning of the measurement interval or just before its end.

Table 1. Parameters of rainfall stages in experiment A

Stage	n [count]	q_I [mm/h]	q_I^* [mm/h]	max r_t [mm]	min r_t [mm]	max q_t [mm/h]	$\mu(q_t)$ [mm/h]	r_I [mm]	t_I [min]	q_I [mm/h]
1	39	50 ± 3%	49	0.204	0.816	52.9	50.7	8.4	10	50.2
2	121	150 ± 3%	156	1.301	2.625	1363.9	278.5	26.9	10	161.3
3	10	6 ± 3%	6	0.000	0.199	6.6	5.6	2.2	20	6.6
4	17	17 ± 3%	16	0.199	0.398	16.2	14.9	3.4	12	16.9
Total	187	–	–	–	–	–	–			

3.2. Experiment B

During the experiment B, a total of 3.5 l of water was poured into the rain gauge in four stages. It is equivalent to 175 mm of rainfall per one square meter, Fig. 6. In the first three stages, 1 l was added, and in each subsequent stage the water flow rate was increased. In the fourth stage, the flow was reduced to a minimum and 0.5 l of water was introduced. Knowing the active surface of the rain gauge, the volumetric condition of each stage was scaled to the amount of precipitation in mm/m2, Tab. 2.

Fig. 6. Experiment stand B – rainfall simulated using dropper

The recorded total rain after four stages was 164.8 mm, that is 6% less than introduced 'rain', Fig. 7. The flow rate in each stage was not constant due to the decreasing height of the water column, which is reflected in recorded values of current rain, Fig. 8. Calculated rainfall intensities indicated that all simulated rainfall events, except the last one, represents a naval rain / violent rain (Met Office 2007). In the first two stages, a very good agreement between the set and measured precipitation amounts was achieved. The measurement errors were 1% and 5%, respectively. In the third

Table 2. Parameters of rainfall stages in experiment B

Stage	r_I	r_I^*	max r_t	min r_t	max q_t	$\mu(q_t)$	r_I	t_I	q_I
	[l]	[mm]	[mm]	[mm]	[mm/h]	[mm/h]	[mm]	[min]	[mm/h]
1	1	50	0.199	3.354	215.5	169.8	50.4	19	159.2
2	1	50	1.792	6.048	461.2	350.7	47.7	9	317.9
3a	1	50	1.120	12.768	1040.9	813.5	43.9	4	658.2
4b	0.5	25	0.199	0.603	32.9	21.0	22.8	68	20.1
Total	3.5	175	–	–	–	–	164.8	–	–

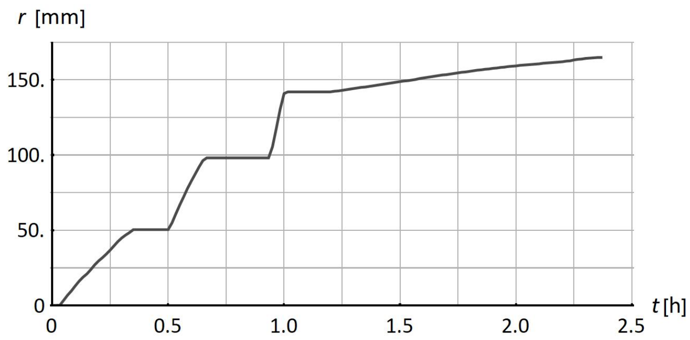

Fig. 7. Total rain compensated time-history simulated during experiment B using dropper

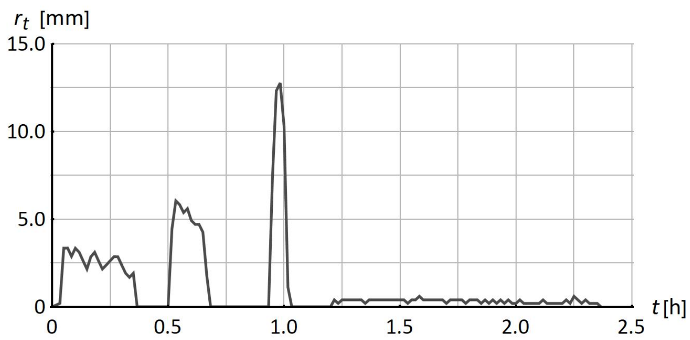

Fig. 8. Current rain time-history simulated during experiment B

stage, the declared limit of rainfall intensity that could be recorded by the device, equal to 600 mm/h, was exceeded. This probably resulted in a larger measurement error of 12%. In the last stage, simulating the least intense rainfall, the recorder showed 9% less rain than poured into the rain gauge.

4. Data Collected

4.1. General Information

In Poland the hydrological year starts in November 1st and ends in October 31st. The station started to collect data in November 18th, 2022, so with a slight delay compared to the beginning of the hydrological year 2023. The total precipitation registered during half year was 107 mm, Fig. 9. According to the methodology used by meteorologists, the amount of rain that fell in the subsequent days, weeks and months of the year is analysed. The rainiest month of this half-year was February 2023, Fig. 10, with total rain equal to 38.1 mm. The most rain, 9.2 mm, fell in the 50th week of 2022, Fig. 11. The maximum daily precipitation occurred on February 20, 2023 and amounted 25.5 mm. Among all daily records, 5 were selected, in which the daily precipitation was higher than 5 mm, Fig. 12. Compared to historical data collected for Poland, where the maximum daily rainfall was 300 mm, or with the 128 mm rainfall that occurred in Gdańsk in 2001 (which caused damage to hydrotechnical facilities and a flood), these were very small rainfalls. There were 96 rainless days in the analysed period.

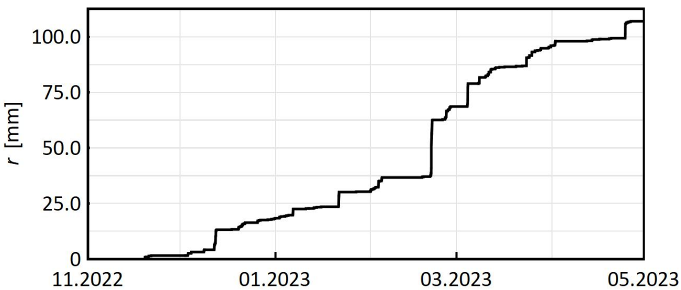

Fig. 9. Total precipitation in first half of hydrological year 2023 (measurements started in November 18th, 2022)

It was assumed that in engineering applications what is interesting is a total rainfall in the considered time period, not the rainfall in a given month or week of the year. Therefore, some conclusions presented in the paper are based on the moving sum of rainfall r_Σ that occurred in the intervals of 3, 7 and 30 days preceding the day of analysis, Fig. 13. The maximum rainfall over a 30-day period, equal to 49.8 mm, was reached on March 16, 2023 and remained at this level for the next 5 days. Before this event, the 30-day sum of rainfall remained at an average level of 15 mm and the average returned to this level at the end of the half-year. Fig. 14 shows different rainfall over 30-days that resulted in almost the same total rain. By analysing the 7-day moving sum, one period with significant values can be identified. Between February 19 and 26, 2023, a total rain of 31.3 mm was recorded. At the beginning of this period, the maximum rainfall for 3-day moving sum was also measured.

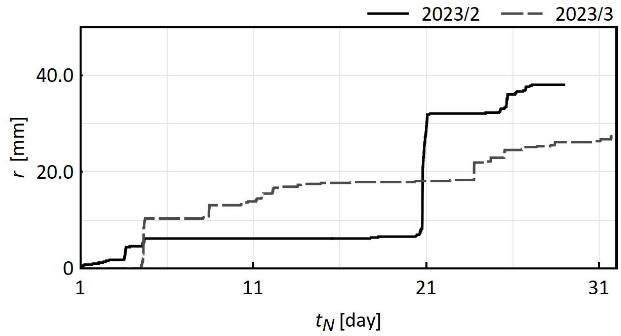

Fig. 10. Pluviograms recorded in February and March of 2023

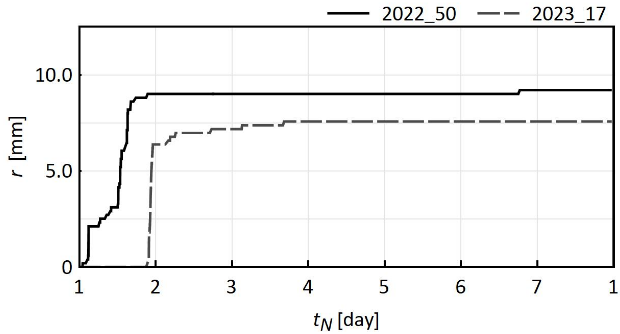

Fig. 11. Pluviograms recored in 50th week of 2022 and 17th week of 2023

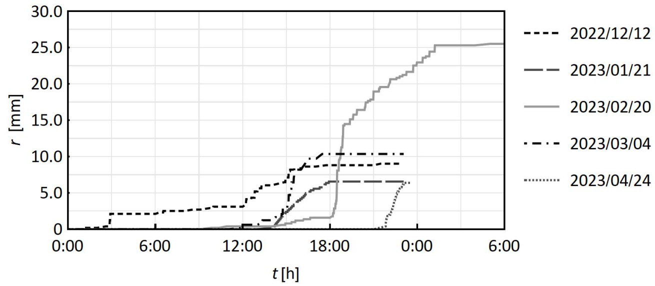

Fig. 12. Total precipitation time-histories in selected days

4.2. Rainfall Model

The proposed procedure for determining the rainfall boundary condition consist of four stages. The starting point is the file included daily records. (a) To ensure the completeness of records of the rainfall event that occurred at night the records of current rain r_t are checked. If the last record of r_t is different from zero, the data are supplemented with the records from the next day. (b) In the second stage the rainfall event I is

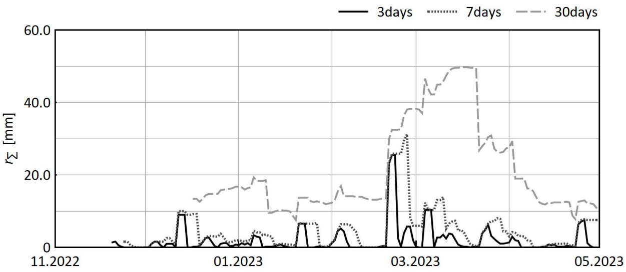

Fig. 13. Moving sum of precipitation in first half of hydrological year 2023

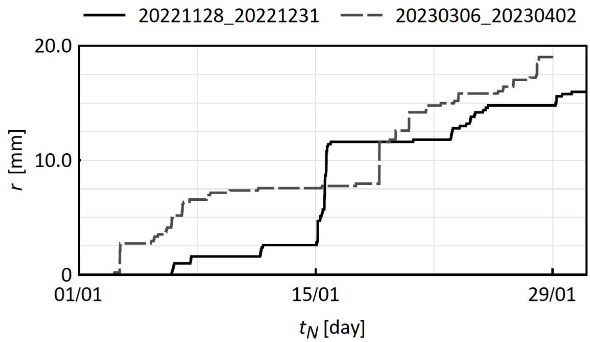

Fig. 14. 30-days pluviograms with the same total rain

extracted form daily records. Firstly, the time of occurrence of the maximum rainfall intensity is determined, and then fragments of the daily data with rainfall breaks exceeding 1 hour are removed. It is not known, whether the bucket was empty or filled before the first impulse. Therefore, it is assumed that the first filling of the bucket took 15 minutes, the zero of normalised time t_N of the rainfall event is set. The final fragment of the recording in which there is no increase in precipitation is also omitted. After such processing, the total rainfall r_I, duration d_I and average intensity q_I of the selected event I are determined. (c) In the next stage, the rainfall time-history $r(t_N)$ is approximated at equal time intervals of 1 minute using the moving least squares method. It is now possible to calculate the rainfall derivative equivalent to the rainfall intensity expressed in mm/h. The maximum values of the current intensity, max q_t, and the maximum current precipitation max r_t are calculated. (d) The last stage of processing consists in indicating time intervals characterized by constant rainfall intensity.

The five one-day rainfall events were selected in the previous section for further processing. They were selected based on the highest value of daily rain. The pluviograms processed according to the procedure described above are shown in the Fig. 15. The most intense rainfall event, characterised by maximum average intensity of

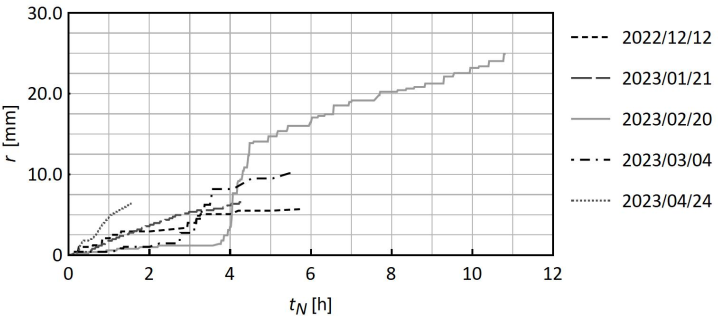

Fig. 15. Modified pluviograms of selected precipitation events (total daily rain higher than 5 mm)

Table 3. Parameters determined for selected precipitation events

Date	max q_t [mm/h]	max r_t [mm]	q_I [mm/h]	r_I [mm]	t_I [h]	$t_{\max qt}$ [h]	Stages
2022/12/12	38.8	0.647	1.0	5.7	5.8	3.2	4
2023/01/21	3.0	0.199	1.5	6.6	4.3	0.4	1
2023/02/20	106.1	1.768	2.3	24.9	10.8	4.1	3
2023/03/04	65.7	1.095	1.9	10.2	5.5	3.2	3
2023/04/24	22.9	0.381	4.2	6.4	1.5	0.3	2

4.2 mm/h (Tab. 3), occurred on April 224, 2023. During 1.5 hour felt almost the same amount of water as in January 21th, 2023 in 4.3 hours. Both events, representing moderate and light rainfall, can be modelled using one stage. The longest rainfall event lasting 10.8 hours and resulting in total rain of 24.2 mm occurred on February 20th, 2023. This event can be modelled using three stages with various intensities of 0.9 mm/h; 9.5 mm/h and 1.8 mm/h and lasting 4 h, 1.1 h and 5.6 h, respectively. The middle part can be described as heavy rain.

5. Conclusions and Perspectives

The article presents the characteristics and results of the tests conducted on the rain gauge by DeltaOHM with pre-set configuration. The test results allowed us to understand the recorded variables. It was found that all recorded variables are modified by internal procedure based on the calibration curve. It was shown that the maximum intensity values given by the recorder may contain errors. Therefore, rainfall event classification based on these value would not be correct. Recorded max rainfall rate time-history cannot also be used directly as boundary conditions in numerical simulations. Despite the direct availability of various forms of measurement results, it is recommended to use the current rain or total rain records in further analysis.

In the paper, the data recorded in the first half of the hydrological year 2023 are analysed. In the analysed period, the maximum daily amount of precipitation occurred on February 20th, 2023 and was equal to 25.5 mm. The maximum total rainfall over a 30-day period, equal to 49.8 mm, was achieved on March 16h, 2023. A period with significant 7-day total values occurred between February 19th and 26th, 2023, when a total rainfall of 31.3 mm was recorded. The first rainfall models for the Wiślinka region that would be applied into numerical simulations was presented. The duration of selected events ranged from 1.5 to 10 hours. The parameters of two single-stage events representing a moderate and light rainfall model were defined. One of the multi-stage events includes a heavy rain lasting 1.1 hours. I am convinced, that after several years of observation, it will be possible to present reliable rainfall patterns for one-day and multi-day rainfall events.

It is also planned that in the future the station will ultimately monitor simultaneously rainfall, ground water content and displacement.

Acknowledgments

The author is grateful for the financial support of the project "Safety assessment of phosphogypsum waste heap in Wiślinka, Poland" provided by the Provincial Fund for Environmental Protection and Water Management (Gdansk, Poland) (www.wfos.gdansk.pl).

References

Alonso E., Gens A., Lloret A., Delahaye C. (1996) Effect of rain infiltration on the stability of slopes, *Proc. 1st Int. Conf. on Unsaturated Soils*, UNSAT '95, Paris, 241–249.

Bednarczyk Z. (2018) Identification of flysch landslide triggers using conventional and 'nearly real-time' monitoring methods – An example from the Carpathian Mountains, Poland, *Engineering Geology*, **244**, 41–56 (doi.org/10.1016/j.enggeo.2018.07.012).

Cai F., Ugai K. (2004) Numerical analysis of rainfall effects on slope stability, *International Journal of Geomechanics (ASCE)*, **4**(2), 69.

Corominas J., Moya J. (1999) Reconstructing recent landslide activity in relation to rainfall in the Llobregat River basin, Eastern Pyrenees, Spain, *Geomorphology*, **30**(1–2), 79–93 (doi.org/10.1016/S0169-555X(99)00046-X).

DeltaOHMa, *Operating manual. Cloud Platform*, (PDF v1.3. retrieved on November 3, 2022).

DeltaOHMb, *Operating manual. Tipping bucket rain gauge HD2015*, (PDF v1.2. retrieved on July 14, 2022).

DeltaOHMc, *Operating manual. Weather station data logger HD33[L]MT.4*, (PDF v4.1. retrieved on August 22, 2022).

Met Office, *Fact Sheet No. 3. Water in atmosphere*, National Meteorological Library and Archive, www.metoffice.gov.uk (PDF published in August 2007, retrieved on September 10, 2022).

Suradi M., Fourie A. (2014) The effect of rainfall patterns on the mechanisms of shallow slope failure, *Aceh International Journal of Science and Technology*, **3**(1), 1–18, (doi: 10.13170/AIJST.0301.01).

Świtała B., Wu W. (2019) Simulation of Rainfall-Induced Landslide of the Vegetated Slope, [In:] Wu W (ed.), *Recent Advances in Geotechnical Research*, Springer Series in Geomechanics and Geoengineering, 187–196. (doi:10.1007/978-3-319-89671-7_16).

WMO (2014) *Guide to Meteorological Instruments and Methods of Observation. Measurement of Precipitation*, (WMO-No. 8) Part I (Eighth ed.), World Meteorological Organization, 2014, (PDF retrieved on June 10, 2022).

Zabuski L., Świdziński W., Kulczykowski M., Mrozek T., Laskowicz I. (2015) Monitoring of landslides in the Brda river valley in Koronowo (Polish Lowlands), *Environmental Earth Sciences*, **73**, 8609–8619, (DOI 10.1007/s12665-015-4025-3).